Solvent Effects on the Intramolecular Hydrogen−Atom Transfer between Tyrosine and Benzophenone. Diverting Reaction Mechanisms in Protic and Nonprotic Media†

ARTICLE *in* THE JOURNAL OF PHYSICAL CHEMISTRY C · JULY 2009

Impact Factor: 4.77 · DOI: 10.1021/jp901740z

Solvent Effects on the Intramolecular Hydrogen-Atom Transfer between Tyrosine and Benzophenone. Diverting Reaction Mechanisms in Protic and Nonprotic Media†

Gerald Hörner,* Anna Lewandowska, Gordon L. Hug,‡ and Bronislaw Marciniak

Faculty of Chemistry, Adam Mickiewicz University Poznan, Grunwaldzka 6, PL-60-780 Poznan, Poland

Received: February 25, 2009; Revised Manuscript Received: May 5, 2009

The intramolecular hydrogen-atom transfer between tyrosine and triplet-excited benzophenone was studied by nanosecond laser-flash photolysis in a number of nonprotic and protic solvents. The reaction rates were found to be strongly solvent dependent with a range from $<10^5$ s^{-1} to 5×10^7 s^{-1}. Eventual contributions from solvent-dependent conformational equilibria on the reaction rates were found to be of minor importance. In contrast, the rate-enhancing and rate-retarding effects of the solvents could be attributed to specific solvent−solute interactions with the hydrogen donor and the hydrogen acceptor. Opposite effects were exerted by nonprotic and protic solvents. The sharp decrease of the reaction rates in nonprotic solvents with the hydrogen-bond acceptor ability of the solvent is referred to hydrogen bonding of the tyrosine to the solvent, TyrOH → S. It could be quantified in terms of an intramolecular kinetic solvent effect model. In turn, a sharp increase of the reaction rates with the hydrogen-bond donor ability of the solvents is observed in protic solvents, which is referred to solvation effects on both chromophores, SH → O(H)Tyr and SH → bp. Implications of these diverting solvent dependencies on the reaction mechanism in protic and nonprotic solvents are discussed.

Introduction

Phenols play fundamental roles in biology due to their greatly reversible redox chemistry. The propensity of phenols to act as a chain-breaking agent or antioxidant in the radical-induced peroxidation of organic compounds is as well established as the vital role of the tyrosine/tyrosyl radical couple in the active center of numerous enzymes.[1] The chain-breaking ability of phenols is generally referred to the ease of the donation of the phenolic hydrogen atom (H-atom) to the attacking radical. As a net effect one hydrogen atom is transferred from the donor to the acceptor. Currently there is much debate about the actual mechanism of this net single-step H-transfer, that is, whether the proton and the electron transfer employ the same orbital or different orbitals of the acceptor.[2] For the former case the notation hydrogen-atom transfer (HAT) has been recommended, whereas in the latter case the notation of a proton-coupled electron transfer (PCET) is chosen.[2a] In this work we will not distinguish between a HAT and a PCET pathway. The notation HAT will be chosen whenever a single-step transfer is inferred from the experimental data. In contrast, the notation stepwise electron-transfer proton-transfer (ET-PT) is reserved for an electron-transfer initiated reaction.

Unlike other radical reactions[3] the H-atom transfer from phenols is strongly dependent on the solvent. In particular, extensive work by Ingold and Lusztyk has provided evidence that the dramatic deactivation of phenolic antioxidants in strongly associated media can be attributed to hydrogen-bonding of the phenol to the solvent.[4] The model of a kinetic solvent effect (KSE) which was deduced from these studies is based on a H-bond equilibrium (phenol···solvent) in a simple predissociation kinetic scheme. The solvent dependence of the reaction rate constants was quantified solely in terms of the H-bond donator ability of the H-atom donor (here the phenol) and the H-bond acceptor ability of the solvent. An important implication of this model is that the nature of the attacking radical, which implies also its solvation properties, has no impact on the KSE. It is noted that, intrinsically, the KSE model makes no difference between an underlying HAT pathway and a PCET pathway.[4h]

Although the KSE concept was successfully applied in the interpretation of radical reactions of other donors also (e.g., amines),[5] it is noted that recent studies on the H-atom transfer quenching of triplet-excited acceptors cast some doubt on the general applicability. Therein a KSE was observable also for donors without any tendency to form H-bonds.[6] The contrasting successful description of the H-atom transfer quenching of a triplet-excited ketone by phenols[7] shows that this possible failure of the KSE concept is not due to a general nonapplicability in the excited state (triplet states are commonly taken to be radical-like in nature[8]). In agreement with this conclusion, we could recently refer the solvent dependence of intramolecular H-atom transfer systems (benzophenone-tyrosine dyads, bp∪Tyr) to effects of H-bonding of the phenol to the solvent within a predissociation kinetic scheme which was extended to include the molecular dynamics.[9] This success is somehow surprising, since the propensity of benzophenone and its triplet state to form H-bonds is well established and interference with the phenol-based KSE might have been expected. Therefore, a puzzling detail remains to be addressed: Is the chemical nature and, especially, the solvation behavior of the acceptor insignificant in the case of triplet-excited ketones?

In order to address this question we have extended our nanosecond laser-flash photolysis (LFP) studies on the intramolecular H-atom transfer reactions in triplet-excited bp∪Tyr dyads with variable donor−acceptor geometries. From former work it was known that the nature of the solvent exerts a strong effect

† Part of the "Hiroshi Masuhara Festschrift".

* To whom correspondence should be addressed. Fax: (+48) 61-829-4367. E-mail: hoerner@amu.edu.pl.

‡ Fulbright Scholar at AMU. Permanent address: Radiation Laboratory, University of Notre Dame, South Bend, IN.

10.1021/jp901740z CCC: $40.75
Published on Web 05/28/2009

SCHEME 1: Structure of the Dyad 1, Based on 3-Benzoylbenzoic Acid (3-bpc) and (*S*)-Tyrosine Methylester and Photoinduced Formation of the Biradical 3 via Intramolecular Hydrogen-Atom Transfer in 1

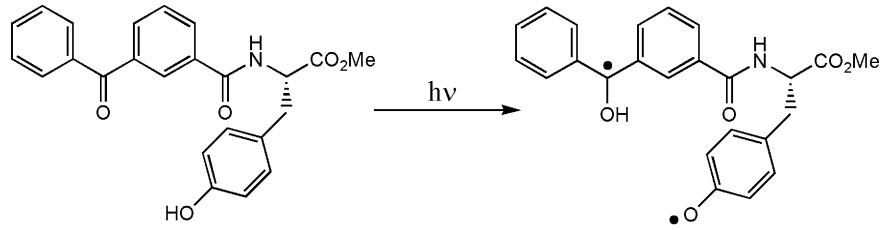

1: 3-bpc-(*S*)-Tyr-OMe **3**

on the H-atom transfer rate constants, $k_H^{(S)}$, of the benzamide-bound dyad **1** (Scheme 1).[10] H-atom transfer in this dyad differed by a factor of 40 in dichloromethane (DCM) and acetonitrile (ACN) solutions. Here we report the solvent dependence of the intramolecular H-atom transfer quenching of the dyad **1** in eighteen different solvent and solvent mixtures. The time-resolved studies are supplemented by NMR and DFT studies with a view on the conformational aspects of the reaction. Different from the previous study, two solvent parameters were found necessary to account for the solvent dependence of the reaction rates, namely the effective H-bond acceptor ability, $\Sigma\beta_2^H$, and the effective H-bond donor ability, $\Sigma\alpha_2^H$, as defined by Abraham et al.[11] The consequences of this finding for the respective reaction mechanisms in protic and nonprotic solvents are discussed.

Experimental Section

General. Synthesis of the dyad **1** followed the routines of carbodiimide-induced amide coupling, as previously described in detail.[10] Routine ^{1}H and ^{13}C NMR spectra (200 and 50.32 MHz, respectively) were recorded in deuterated solvents and are reported in ppm downfield from TMS.

Laser Flash Photolysis (LFP). The two set-ups for laser flash photolysis have been described in detail previously.[12] LFP is based on the 266 or 355 nm output of a Nd:YAG laser in both cases, with a full width at half-maximum of ca. 7 or 9 ns and a dose of 5−7 or 7−12 mJ pulse^{-1} at 266 or 355 nm, respectively. Neutral filters were used for attenuation of the laser intensity at high dyad concentrations. Dyad concentration and laser intensity were adjusted to keep the initial concentration of transients between 15 and 30 μM. Transient concentrations were calibrated by relative actinometry (^{3}bp in ACN). Transient decays were recorded at individual wavelengths by the step-scan method with a step distance of 5 nm in the range of 300 to 850 nm and obtained as the mean signals of 6 to 16 pulses. Spectral resolution was in the range of ±3 nm. Samples for LFP were rigorously deoxygenated by flushing with analytical grade nitrogen for 20 min prior to and kept under nitrogen during measurement in sealed quartz cuvettes. Alternatively samples were irradiated in a circulating flow system (5 × 5 mm Suprasil cuvettes). Samples were prepared from millimolar stock solutions by dilution. LFP experiments were performed at 295 ± 1 K. Experiments in neat *tert*-butanol and in *N*-methylacetamide/acetonitrile 25:1 (vol./vol.) were performed at 300 ± 1 K to avoid freezing of the samples. Solvents for time-resolved spectroscopy were of the highest available analytical grade and were used without further purification.

Computational Details. All calculations in this work were performed by the Gaussian 03 program. The hybrid functional of Perdew, Burke and Ernzerhof PBE1PBE was used. Geometry optimization and energy calculations were carried out using the standard 6-31G basis set. This basis set offers a reasonable compromise between the proper description of the species and good performance at a modest computational cost. Our aim was to find the most stable conformers in the ground state for our dyad **1**. DFT calculations for the gas phase show that three rotational isomers g+, g−, and t can adopt structures with similar energy.

Results

LFP: Spectral and Kinetic Analysis. Excitation of the bp chromophore of the dyad **1** yields the excited triplet state **2** with unit quantum yield within the duration of the laser flash. The transient spectrum of the triplet state **2** is readily identified as the dominating intermediate in the early transient spectra ($t <$ 50 ns after the flash) by its characteristic absorption maxima at 325 nm ($\varepsilon_{325} = 14\,000 \pm 2000$ cm^{-1} M^{-1}) and 530 nm ($\varepsilon_{530} = 6500 \pm 1000$ cm^{-1} M^{-1}) and a long-wavelength absorption tailing toward the NIR region. Molar absorption coefficients of **2** were obtained by relative actinometry with absorption-matched solutions of bp in ACN (ε_{530} (bp) $= 6500 \pm 500$ cm^{-1} M^{-1}).[13] Exceptional behavior is noted during LFP of hexafluoro-2-propanol (HFIP) solutions of **1** and bp, where an additional absorption band became evident at 400 nm. Besides that, absorption coefficients and band positions of **2** showed only little variation with change in the solvent.

In contrast, the time evolution of the transient spectra is strongly dependent on the nature of the solvent. This is illustrated by transient spectra observed at 200 ns for diluted solutions in ethyl acetate (EtOAc), acetonitrile/water 10:1, and 1,2-dichloroethane (DCE) (Figure 1a). The marked absorption loss around 530 nm and an additional feature at 405 nm in the case of the ACN/H_2O and DCE is readily explained by the formation of the benzophenone ketyl radical (bpH$^\bullet$; $\varepsilon_{550} = 2900 \pm 300$ cm^{-1} M^{-1}) and the tyrosyl radical (TyrO$^\bullet$; $\varepsilon_{405} = 1900 \pm 200$ cm^{-1} M^{-1}), concomitant with triplet decay. The observed spectral evolution is reflected by the solvent dependence of the decay rate constants of **2**, k_D. These were extracted from monoexponential fits to the experimental decay profiles at 630 nm (typical profiles are shown in Figure 1b). At this wavelength only the triplet state has significant absorption since the formation of the benzophenone ketyl radical anion, with a strong absorption at 630 nm, proved to be insignificant throughout this study (except in methanol/sodium methanolate). The values obtained have been cross-checked by biexponential fits to the profiles at 510 nm, where the second decay component is referred to the biradical **3** (see below). Agreement between both methods was usually within 5%.

The gross decay-rate constant, k_D, is the result of several competing pathways as summarized in Scheme 2 and eq 1.

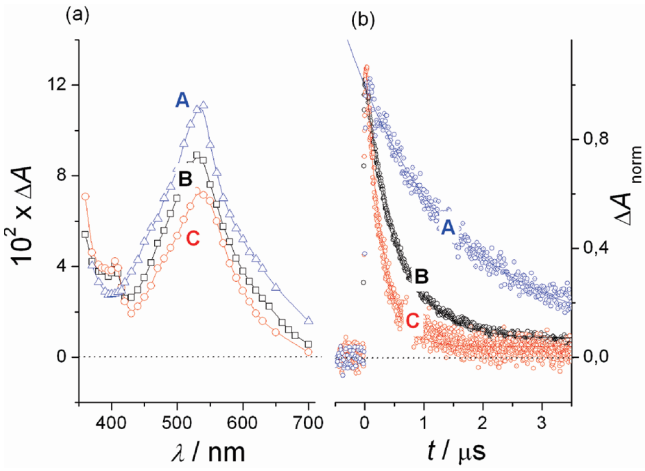

Figure 1. (a) Transient absorption spectra obtained 200 ns after laser flash photolysis (355 nm; 12 mJ pulse^{-1}) and (b) normalized decay profiles observed at 630 nm for solutions of **1** (0.2 mM < [**1**] < 0.4 mM) in (A) ethylacetate (blue), (B) acetonitrile/water 10:1 (*v*/*v*) (black), and (C) 1,2-dichloroethane (red); lines: exponential fits to the experimental data; initial triplet concentration $[T]_0 = 15-20$ μM.

SCHEME 2: Deactivation Paths of the Triplet-Excited State 2 of the Dyad 1[a]

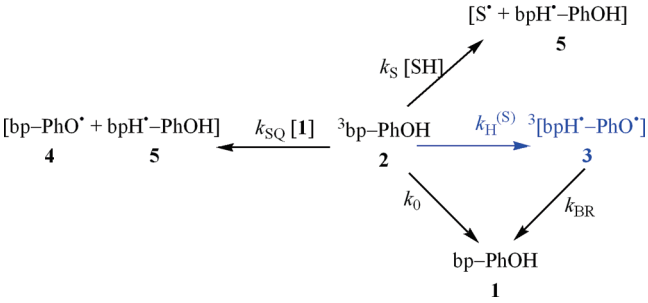

[a] The superscript (S) in $k_H^{(S)}$ denotes the solvent dependence of this rate constant in contrast to the solvent-independent k_H^0; see below.

Three parallel pathways for the formation of free radicals can be identified and separated, that is, intramolecular hydrogen-atom transfer, hydrogen-atom abstraction from the solvent, and self-quenching by ground-state **1**. Each of these contributions is found to be solvent dependent.

$$k_D = k_H^{(S)} + k_0 + k_S[SH] + k_{SQ}[\mathbf{1}] \qquad (1)$$

In agreement with the previously reported LFP results of **1** in ACN, methanol (MeOH), and dichloromethane (DCM),[10] the values for k_D were found to be strongly concentration dependent in most of the solvents. This behavior is due to contributions from bimolecular quenching of **2** by ground-state **1** governed by the rate constant k_{SQ}. Self-quenching affords the ketyl radical **5** and the tyrosyl radical **4**. These species decay by bimolecular processes within tens of microseconds and therefore give a virtually constant offset in the transient-decay time profiles on the time scale of the experiment. Stern−Volmer analysis has been performed to quantify the self-quenching pathway and to eliminate the concentration dependence.

Plots of the concentration-dependent rate constants gave convincingly linear plots with the dyad concentration [**1**] in all cases (not shown), giving the self-quenching rate constants as the slopes of these plots. The observed peculiarities of the solvent dependence of k_{SQ} are not at the center of this study and will be discussed elsewhere. The concentration-independent (ci) decay pathways are characterized by the intercepts of the Stern−Volmer plots with $k_{ci} = k_0 + k_S[SH] + k_H^{(S)}$. They are made up by contributions from the intramolecular HAT pathway, leading to the biradical **3** with the rate constant $k_H^{(S)}$ and the natural decay constant of the bp chromophore in the respective solvent $k_T = k_0 + k_S[SH]$. The contributions can be separated when values for k_T are known.

$$k_H^{(S)} = k_{ci} - (k_0 + k_S[SH]) = k_{ci} - k_T \qquad (2)$$

Values for k_T were accessible by experiments with the reference compound benzophenone in the respective solvents. The range of values from $<10^5$ s^{-1} in ACN and water to 10^7 s^{-1} in an *N*-methylacetamide/ACN mixture mainly reflects the ability of the solvent to act as an H-atom donor to the bp triplet (Table 1). Transient spectra revealed that the triplet decay of bp is connected with efficient ketyl-radical formation especially in MeOH and *N*-methylacetamide/ACN, whereas benzonitrile and ACN are virtually inert toward bp.

The rate constants for the intramolecular HAT $k_H^{(S)}$ as calculated by eq 2 cover a range from $<2 \times 10^5$ s^{-1} in EtOAc to 5×10^7 s^{-1} in water/*tert*-butanol (see Table 1). It is noted that the uncertainty of the such-derived rate constants increases significantly with the contributions from H-abstraction from the solvent. Evidently, there is no simple correlation of the rate constants $k_H^{(S)}$ with any of the solvent parameters given in Table 1. High rate constants are generally accompanied by significant spectral contributions of the biradical **3**. First-order decay of this species can be observed at the absorption maxima of the underlying bpH• and TyrO• chromophores at 335 and 405 nm, respectively. A return-HAT step after intersystem crossing to the singlet state cleanly yields back the ground-state dyad **1** with rate constants k_{BR} ranging from 5×10^5 to 2×10^6 s^{-1}.

The high reactivity of **2** obtained in methanol solution in the presence of high concentrations of NaOMe can be readily explained by a simple electron transfer (ET) reaction from the Tyr phenolate ion to the bp triplet. The phenolate anion resulting from the complete deprotonation of the tyrosine phenol is known to be a much better electron donor than the original phenol.[14] Accordingly, transient spectra are made up solely by the strong absorption of the benzophenone ketyl radical anion around 630 nm besides the characteristic feature of the TyrO• around 405 nm. The rate constant in this solvent system is taken as a reference value for a pure ET reaction of the dyad **1** in a solvent of high permittivity.

DFT Studies of the Molecular Structures of the Dyad 1. The structural demand on the dyad **1** to achieve a suitable geometry for the HAT step has been addressed by DFT methods. It is well established, that hydrogen-atom transfer reactions, initiated by triplet-excited ketones demand the close contact between the H-atom donor and the accepting carbonyl moiety.[15] Recent work on the molecular dynamics of the dyad **1** revealed that the probability of close contacts, that is, distances between the remote tyrosine phenol and the benzophenone carbonyl below 3.1 Å, is limited by the directivity and stiffness of the benzamide linker.[10] In the present study, the chemical structures were addressed, that are capable of close contacts and therefore could be taken as models for the quenching geometry.

DFT calculations on the PBE1PBE level of theory with the common 6-31G basis set have been undertaken to access the relative energies of molecular conformations of the dyad **1** in the gas phase. Structural search by energy minimizing was

TABLE 1: Summary of Solvent Parameters and of the Kinetic Data of the Dyad 1

	solvent parameters				rate constants	
	ε_{solv}[a]	η/cp[a]	A[b]	B[b]	$k_H^{(S)}$[c]	k_T[d]
(1) chloroform	4.81	0.537	0.15	0.02	6.9	1.2
(2) ethyl acetate	6.08	0.423	0.00	0.45	<0.2	0.8
(3) acetic acid	6.20	1.056	0.61	0.44	1.7	<0.1
(4) *n*-butylchloride	7.28	0.422	0.00	0.10	4.0[e]	1.1
(5) dichloromethane	8.93	0.413	0.10	0.05	3.2	0.9
(6) 1,2-dichloroethane	10.42	0.779	0.10	0.11	2.9	0.4
(7) *tert*-butanol	12.47	4.312	0.31	0.60	0.7	0.3
(8) hexafluoro-2-propanol	16.70	1.021	0.77	0.10	20.0[f]	0.2
(9) benzonitrile	25.9	1.267	0.00	0.33	*0.3*	0.9
(10) trifluoroethanol	27.68	1.8[g]	0.57	0.25	7.9	0.22
(11) methanol	33.00	0.544	0.43	0.47	*1.2*	6.25
(a) [D_4]-methanol					1.7[f]	1.25
(b) methanol/NaOMe (0.5 M)					>100[f]	
(12) acetonitrile	35.94	0.369	0.07	0.32	*0.3*	<0.1
(13) water	80.10	0.890	0.82	0.35	n.d[h]	<0.1
(a) water/acetonitrile 1:10 (v/v)	≈40[i]		0.54[j]	≈0.34[k]	2.5[f]	
(b) water/acetonitrile 1:2 (v/v)	≈51[i]		0.65[j]	≈0.34[k]	7.1[f]	
(c) water/*tert*-butanol 10:1 (v/v)	≈72[l]	≈1.35[l]	≈0.75[k]	≈0.38[k]	50[f]	
(14) *N*-methylacetamide[m]	179.0	1.28	0.40	0.78		
(a) *N*-methylacetamide/acetonitrile 25:1 (v/v)	≈169[k]		≈0.38[k]	≈0.75[k]	*2.2*[f]	10

[a] At 25 °C; CRC Handbook of Chemistry and Physics, CRC Press, Boca Raton, 76th Ed., 1995. [b] $A = \Sigma\alpha_2^H$; $B = \Sigma\beta_2^H$; taken from ref 11. [c] Obtained from Stern−Volmer plots (see text); in 10^6 s^{-1}; experimental error ± 10%; data in italics: experimental error ± 30%. [d] Taken from experiments with bp; $k_T = k_S \times [SH] + k_0$ (see Scheme 2); in 10^6 s^{-1}; experimental error ± 10%. [e] Single-concentration experiment at λ_{exc} = 266 nm. [f] Single-concentration experiment at λ_{exc} = 355 nm; self-quenching contributions estimated with $k_{SQ} = 7 \times 10^8$ M^{-1} s^{-1}. [g] Taken from: Sierra, P. S.; Tejuca, C. C.; Garcia-Blanca, F. *Helv. Chim. Acta* **2005**, *88*, 312−324. [h] Not determined due to limited solubility. [i] Interpolated from data in: Jellema, R.; Bulthuis, J.; van der Zwan, G. *J. Mol. Liquids* **1997**, *73,74*, 179−183. [j] Interpolated and normalized to the $\Sigma\beta_2^H$ scale from data in: Marcus, Y.; Migron, Y. *J. Phys. Chem.* **1991**, *95*, 400−406. [k] Linear interpolation from data in pure solvents, weighted by molar fractions. [l] Interpolated from data in: Ansari, A. A.; Islam, M. R. *Can. J. Chem.* **1988**, *66*, 1223−1228. [m] Acetonitrile added to avoid freezing of the solution.

performed for three side-chain conformers of tyrosine, g−, t, and g+, that are defined by the C^{α}-C^{β} dihedral angles of −60°, +180°, and +60°, respectively. In addition, two different relative orientations of the carbonyl groups attached to the benzophenone moiety, *syn* and *anti*, have been considered. The results of these calculations are summarized in Figure 2.

The energies of the four lowest-energy structures (**I**−**IV**; depicted in Figure 2b) are found to be in close proximity (ΔE < 2 kcal mol^{-1}). With a view to the intrinsic uncertainties of the DFT method[16] the energy differences are taken to be nonsignificant. Importantly, low-energy structures are accessible for each of the three side-chain conformers. This is in full agreement with experimental data of numerous Tyr derivatives that indicated the simultaneous presence of all three conformers although the relative populations were solvent-dependent (see also below).[17] Notably, among the four low-energy structures there is only one showing an oxygen−oxygen distance within the quenching limit of 3.1 Å (a second close-contact structure is discarded due to high energy). It appears reasonable to conclude that the HAT step can only occur in the g− conformational subspace and that in any other conformation, intramolecular dynamics have to precede the reaction. The solvent dependence of the population of this conformer will be discussed in the following section.

Solvent Dependence of the Molecular Conformations. As an important result of the NMR studies on the molecular conformations it is noted that the overall effect of solvent variation on the molecular conformations is only weak. In particular, no differences were observed between protic and nonprotic solvents. The dyad **1** was probed by NMR with respect to the side-chain conformations of the Tyr residue. Information about the side-chain conformations of aromatic amino acids is accessible via the vicinal coupling constants between the diastereotopic β-protons and the α-proton of the amino acid side chain, $^3J(H^{\alpha}-H^{\beta R})$ and $^3J(H^{\alpha}-H^{\beta S})$. With a view to the possible correspondence between the solvent effects on the molecular conformations and on the photochemical reactivity, the ^{1}H NMR spectra of **1** have been analyzed in a number of protic and nonprotic deuterated solvents. A part of these data has been reported previously in a study on the regiochemical aspects of the intramolecular HAT.[10]

Populations p_i of the side-chain conformers i = g−, g+, and t (see Figure 2) have been computed from the experimental coupling constants following the method introduced by Pachler.[18] The conformations g−, t, and g+ were defined with respect to the Tyr side-chain dihedrals, according to the IUPAC conventions. With an error in $^3J(H^{\alpha}-H^{\beta(S/R)})$ of ± 0.2 Hz, the resulting errors in rotamer populations are estimated to be ± 0.03 and ± 0.05 for p_{g-} (p_t) and p_{g+}, respectively. It is noted that the intrinsic uncertainty of the population of g+ is large for small absolute values of p_{g+}.

In agreement with studies on *N*-Ac-Tyr-OMe the population of the conformer t is not affected by the solvent with $p_t \approx 0.27$ (not shown).[17] As previously reported for two bp∪Tyr dyads connected by a more flexible benzylamide linker, the population of g− increases linearly with the permittivity at the expense of the conformer g+, however, with a significantly smaller dynamic range from 0.50 in dioxane to 0.65 in dimethylsulfoxide. The computed populations of the conformers g− (blue symbols) and g+ (red symbols) are plotted against the bulk permittivity of the solvents in Figure 3. Importantly, no peculiarities are observed in the conformer populations of **1** in protic solvents, that is, in methanol, 2-propanol, and acetic acid. In contrast, the data obtained in chloroform and dichloromethane solutions (highlighted in Figure 3) deviate from the general trend. Notably, in both solvents the presumably nonreactive g+ conformer is favored in agreement with the DFT results. The exceptional behavior of the chlorohydrocarbons cannot be

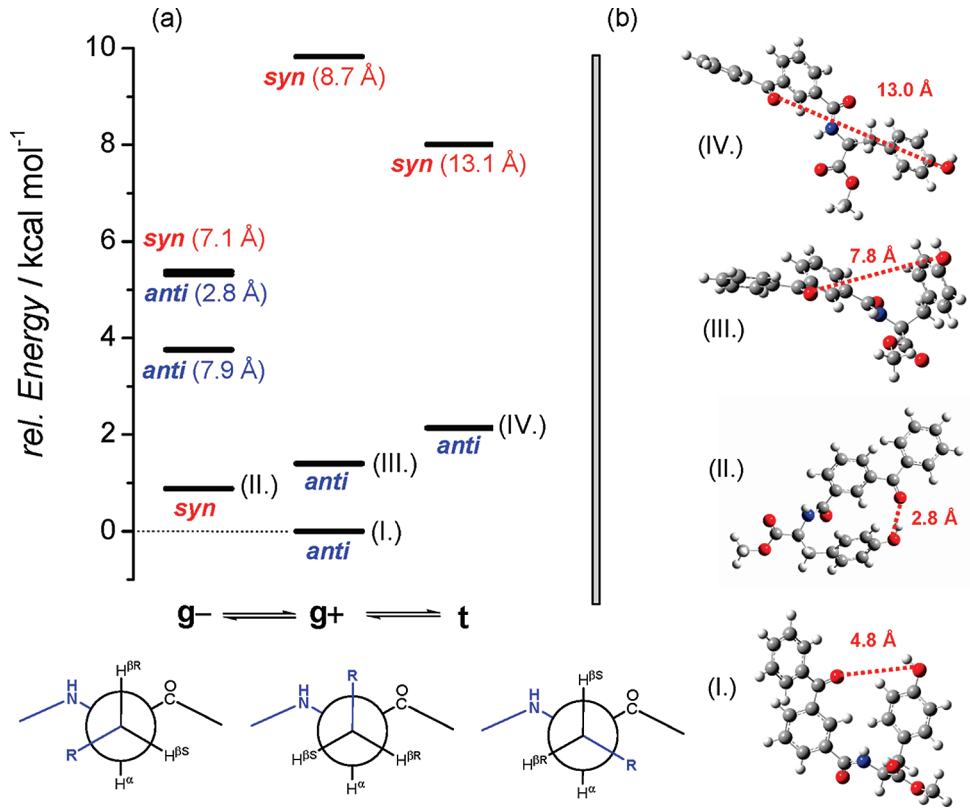

Figure 2. Results of gas-phase DFT calculations (PBE1PBE; 6-31G basis set) of the dyad **1**; (a) energetic order of structures for the Tyr-side chain conformers g−, g+, and t (syn and anti denote the geometry of the two carbonyls on the benzophenone moiety); lower panel: Newman projections of the (*S*)-Tyr side chain along the $C^{\alpha}-C^{\beta}$ bond with R = 4-hydroxyphenyl; (b) "stick-and-ball" structures of the energetic minima **I**−**IV** of the three side-chain conformers; numbers denote the O−O distances between the benzophenone carbonyl and the phenol oxygen.

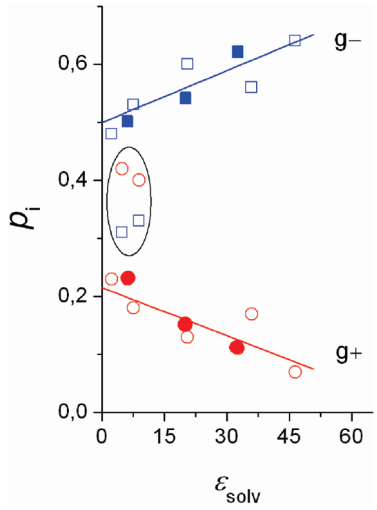

Figure 3. Dependence of the conformer populations p_i of dyad **1** on the bulk permittivity of the solvent; squares: conformer g−; circles: conformer g+; filled symbols: protic solvents; not shown: conformer t with p_t = constant = 0.27 ± 0.02; lines: linear fits to the data.

resolved with the limited experimental data. However, the preference of **1** to form the sterically more crowded conformer g+ in chloroform and dichloromethane might be attributed to the vanishing H-bonding properties of those solvents. H-bonding of the amide backbone to the solvent, as it can be inferred from solvent-dependent downfield shifts of the amide protons, is suggested to disfavor the g+ conformer due to enhanced sterical restrictions.

Discussion

The intramolecular H-atom transfer in the benzamide-linked dyad **1** is found to be strongly solvent dependent with rate constants $k_H^{(S)}$ ranging from $<2 \times 10^5$ to 5×10^7 s^{-1} as summarized in Table 1. In the following sections it will be shown that the solvent dependence cannot be referred solely to solute−solvent interactions of the tyrosine moiety as it was recently reported for a diastereomeric pair of bp∪Tyr dyads.[9] Instead, specific solvent−solute interactions of the tyrosine and the benzophenone moiety have to be considered. Solvent effects on the molecular conformations and intramolecular dynamics appear to be of minor importance.

Hydrogen-Atom Transfer Kinetics of 1. Previous work on the solvent dependence of bimolecular HAT reactions of phenols has revealed that the rate constants are correlated with the H-bonding properties of the solvent.[4] Linear-free energy relationships of the logarithmic rate constants depended solely on Abraham's H-bond acceptor ability, β_2^H,[19] and corresponding plots were found to be linear.[4d] In recent work on the intramolecular HAT reaction between remote bp and Tyr moieties of diastereomeric bp∪Tyr dyads in 15 solvents,[9] we also found one solvent parameter dominating the linear-free energy relationship, namely Abraham's effective H-bond acceptor ability, $\Sigma\beta_2^H$.[11] As an important result, the stereoselectivity of the HAT process was linearly dependent on this parameter, irrespective of the protic or nonprotic character of the solvents.

The present work on dyad **1** shows that the single-parameter dependence of the HAT reactions cannot be generalized in the case of intramolecular reactions. A plot of the kinetic data compiled in Table 1 against the effective H-bond acceptor ability of the solvents exhibits broadly scattered data (Figure 4).

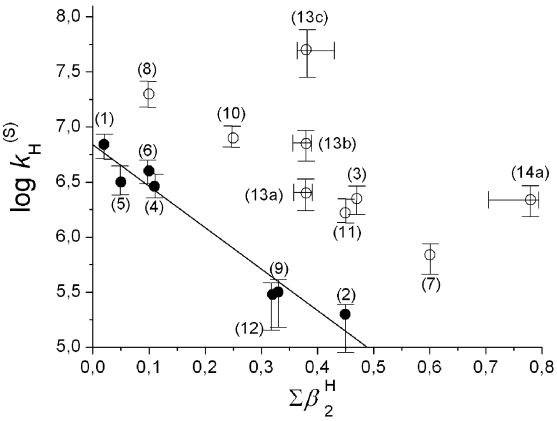

Figure 4. Plot of the H-atom transfer rate constants, log $k_H^{(S)}$ (computed according to eq 2), against Abraham's et al. effective H-bond acceptor ability, $\Sigma\beta_2^H$; open symbols: protic solvents; filled symbols: nonprotic solvents; line: linear regression to the data in nonprotic solvents; solvent code as in Table 1.

Interestingly, two different regions can be identified in the plot with regard to the protic or nonprotic character of the solvents. HAT rates in nonprotic solvents with weak effective H-bond donor abilities $\Sigma\alpha_2^H \leq 0.15$ (filled symbols in Figure 4) are actually found to follow a linear dependence on the $\Sigma\beta_2^H$ values (eq 3) as was observed previously for related dyads.[9] The diminished intramolecular reactivity of **1** in acetonitrile, benzonitrile, and ethyl acetate interfered with kinetic analysis. Therefore the kinetic data in these solvents represent upper limits of the intramolecular HAT rate constants $k_H^{(S)}$. Irrespective of this uncertainty, the slope of the linear dependence in Figure 4 which reflects the H-bond dependence of the HAT rates for **1** with $b = 3.8 \pm 0.3$ is much larger than previously found for another pair of bp∪Tyr dyads with $b = 2.1 \pm 0.1$ and 1.3 ± 0.1.[9]

$$\log k_H^{(S)} = \log k_H^0 - b\Sigma\beta_2^H = (6.8 \pm 0.1) - (3.8 \pm 0.3)\Sigma\beta_2^H \ (N = 7; \text{for } \Sigma\alpha_2^H \leq 0.15) \quad (3)$$

We can rule out significant kinetic effects from solvent-dependent changes of the dyad conformations although the molecular conformations are undoubtedly affected by the solvent properties. As shown before, specific interactions of **1** with H-bond accepting solvents lead preferably to the Tyr side-chain conformation g− (NMR studies, see above). DFT calculations have shown that the conformational subspace of g− also hosts the quenching geometry of **1**. The increasing populations of g− in H-bond accepting solvents as became evident from NMR, however, are not connected with an increase but with a sharp decrease of the HAT rates (linear fit in Figure 4).

The second region in Figure 4 is made up by the protic solvents with significant H-bond donor abilities $\Sigma\alpha_2^H > 0.3$. The protic solvents appear to allow much higher rate constants than their nonprotic counterparts with similar H-bond acceptor abilities. This is illustrated with the example of ethyl acetate and acetic acid that share the same H-bond acceptor ability ($\Sigma\beta_2^H = 0.45$) but which differ in their rate constants by a factor of ≥20. The possible reasons for the diverting behavior in protic solvents will be discussed below.

HAT Reactions in Nonprotic Solvents. Specific Solvation of the Tyrosine Moiety. In nonprotic solvents, the HAT rate constants of **1** show a linear correlation with the H-bond acceptor ability of the solvent; a behavior that is well in accord with the implications of a kinetic solvent effect. The concept of a KSE on the rate of H-atom transfer reactions by specific solvation of the H-atom donor has been elaborated mainly by Ingold and Lusztyk within the past two decades.[4] The long-known rate-retarding effect of H-bond accepting solvents on HAT reactions of phenols therein is ascribed to the reversible masking of the H-atom donor by the solvent making the phenol, in its H-bonded form, inaccessible to the HAT reaction. A predissociation mechanistic model underlies this concept. We recently provided experimental evidence that this concept can be extended toward intramolecular reactions when the molecular dynamics are accounted for.[9]

SCHEME 3: Kinetic Schemes of the Intramolecular H-Atom Transfer in a Three-Step Mechanism

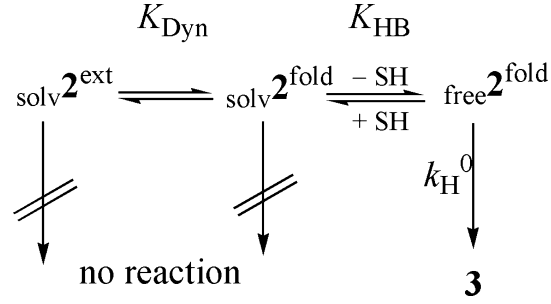

The general idea of this "intramolecular KSE" on the dynamics of the triplet-excited state **2** is depicted in Scheme 3. For the sake of mathematical accessibility this scheme refers to the limits of strong H-bonding with K_{HB} [SH] ≫ 1 ([SH] denotes the molarity of the solvent). In this three-step reaction mechanism the intramolecular motions (folding/unfolding equilibrium K_{Dyn}) and the H-bonding (solvation/desolvation equilibrium K_{HB}) have been included in addition to the isolated HAT step with the rate constant k_H^0. The different triplet species are defined as $_{solv}\mathbf{2}^{ext}$ (solvated/extended), $_{solv}\mathbf{2}^{fold}$ (solvated/folded), and $_{free}\mathbf{2}^{fold}$ (unsolvated/folded). With the assumption of fast H-bond equilibration of $_{solv}\mathbf{2}^{fold}$ and $_{free}\mathbf{2}^{fold}$,[20] the gross rate constant of the overall reaction, $k_H^{(S)}$, in this model is given by eq 4. A detailed derivation of this equation has been given previously.[9]

Equation 4 consists of one H-bond independent and one H-bond dependent part. The former is simply made up by a molecular-dynamics contribution. k_{Dyn}^f denotes the rate constant for dyad folding and, as such, is viscosity dependent. The latter consists of the rate constant of the isolated HAT step, k_H^0, which is scaled by two equilibrium constants for the H-bonding and the folding/unfolding of the dyad. Considering the definition of the latter equilibrium constant, $K_{Dyn} = k_{Dyn}^f/k_{Dyn}^b$, eq 4 can be converted to a logarithmic form that is linear in the H-bonding terms (eq 5).

$$\frac{1}{k_H^{(S)}} = \frac{1}{k_{Dyn}^f} + \frac{K_{HB}[SH]}{K_{Dyn}k_H^0} \quad (4)$$

$$\log k_H^{(S)} = \log k_{Dyn}^f - \log\left\{1 + \frac{k_{Dyn}^b}{k_H^0}K_{HB}[SH]\right\} \quad (5)$$

Notably, the second term on the right-hand side in eq 5 is closely related to the term log{1 + K_{HB}[SH]} which describes quantitatively H-bonding in the bimolecular HAT from H-donors.[4a] As a consequence, both the intermolecular and the

intramolecular model of the KSE imply identical solvent dependences when the scaling factor of $K_{HB}[SH]$ in eq 5 is equal or close to one, that is, when $k^{b}_{Dyn} \approx k^{H}_{0}$. This similarity is of importance, because in a subsequent empirical approach Ingold et al. expressed the H-bonding term $K_{HB}[SH]$, which is problematic to access experimentally, by the tabulated values of the H-bond donor ability of the solute α^{H}_{2} and the H-bond acceptor ability of the solvent β^{H}_{2} (eq 6).[4d] Plots of the logarithmic intermolecular HAT rate constants against $\beta_2{}^{H}$ therefore yield slopes m that are characteristic for each H-donor.

$$\log\{1 + K_{HB}[S]\} \equiv 8.3\alpha^{H}_{2}\beta^{H}_{2} = -m\beta^{H}_{2} \qquad (6)$$

In contrast, we have obtained different slopes in plots of the logarithmic intramolecular HAT rate constants against $\Sigma\beta^{H}_{2}$ for all of the three dyads analyzed so far, although the H-donor was the same in all cases. Preliminary work on six additional dyads points to the possibility of individual slopes for each of them. In terms of the present model of the intramolecular KSE the variability of slopes can be referred to a variation in the ratio of k^{b}_{Dyn}/k^{0}_{H} which is dependent on the dyad structure. It is undoubtedly an important question, whether the molecular dynamics and/or the isolated HAT step are responsible for the expressed structure dependence.

HAT Reactions in Protic Solvents. H-Bond Donation of the Solvents. The sharp decline in the HAT rates with the H-bond acceptor ability of the nonprotic solvents (linear fit in Figure 4) implies negligible intramolecular reactivity ($k^{(S)}_{H} \approx 10^5$ s^{-1}) in solvents with $\Sigma\beta^{H}_{2} > 0.3$, that is, in strongly H-bond accepting solvents. Inspection of Table 1 reveals that with only two exceptions (HFIP and trifluoroethanol TFE) all of the protic solvents in this study exceed this limiting value of $\Sigma\beta^{H}_{2}$ but do allow significant intramolecular reactivity. Obviously, the higher-than-expected rates in protic solvents cannot be explained in terms of the KSE which refers solely to the solvation of the H-atom donor. In a previous study on more flexibly linked bp∪Tyr dyads we had found that solvent-parameters other than the H-bond acceptor ability are insignificant.[9] In striking contrast we now find that the data for **1** are also strongly affected by the H-bond donor ability of the solvent. This becomes most evident from Figure 5, where the kinetic data obtained for **1** are replotted against $\Sigma\alpha^{H}_{2}$. With the exception of four chlorohydrocarbon solvents ($\Sigma\beta^{H}_{2} \leq 0.11$; red symbols) a convincingly linear plot is obtained with a slope $a = 2.9 \pm 0.3$ ($r^2 = 0.969$).

$$\log k^{(S)}_{H} = \log k^{0}_{H} + a\Sigma\alpha^{H}_{2} = (4.9 \pm 0.1) + (2.9 \pm 0.3)\Sigma\alpha^{H}_{2} \qquad (N = 11; \textit{for}\ \Sigma\beta^{H}_{2} \geq 0.12) \qquad (7)$$

This linear-free energy relationship is different from the dependence on the H-bond accepting properties of the solvent (eq 3) in that the correlation of the HAT rates with the H-bond donor properties is positive; that is, the rate constants increase with the strength of the solvent−solute interaction. This is equivalent to a decrease of the activation free energy under the action of a specific solvent−solute interaction. Certainly, this effect of protic solvents cannot be referred to restrictions of the HAT step by the H-bonding as they are assumed in the KSE concept, as these are necessarily increasing the activation free energy.

The diverging solvent dependencies of HAT in **1** raise the question whether or not the same mechanism is employed in protic and nonprotic solvents. In this respect, it is important to

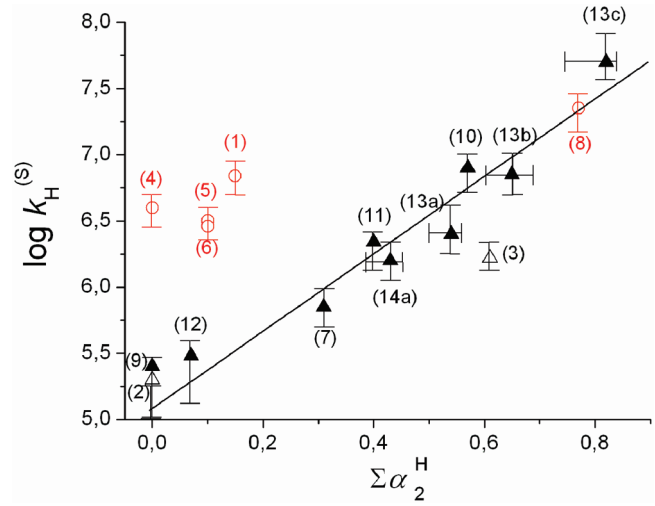

Figure 5. Plot of the H-atom transfer rate constants, log $k^{(S)}_{H}$, against Abraham's et al. effective H-bond donor ability, $\Sigma\alpha^{H}_{2}$; filled symbols: solvents with a bulk permittivity $\varepsilon_{solv} > 10$; open symbols: solvents with a bulk permittivity $\varepsilon_{solv} < 10$; black: solvents with $\Sigma\beta^{H}_{2} \geq 0.25$; red: solvents with $\Sigma\beta^{H}_{2} \leq 0.11$; line: linear fit to the data in high-permittivity solvents (filled symbols); solvent code as in Table 1.

note that the intercepts of the single-solvent parameter regressions in Figures 4 and 5 differ by almost 2 orders of magnitude ($\log k^{0}_{H} = 6.8$ and 4.9 for eqs 3 and 7, respectively). The latter values represent the isolated and solvent-independent HAT rate constants $\log k^{0}_{H}$ and thus should be invariant for a given compound. The observed variance thus is incommensurable with a common mechanism of the H-atom transfer of **1** in protic and nonprotic solvents. To further validate this conclusion, a linear-free energy relationship including both solvent descriptors, that is, the H-bond basicity and the H-bond acidity at the same time was tried (eq 8). The corresponding free-energy relationship and the fit parameters a and b are given in eq 9.

$$\log k^{(S)}_{H} = \log k^{0}_{H} - b\Sigma\beta^{H}_{2} + a\Sigma\alpha^{H}_{2} \qquad (8)$$

$$\log k^{(S)}_{H} = (6.32 \pm 0.14) - (1.72 \pm 0.35)\Sigma\beta^{H}_{2} + (1.81 \pm 0.25)\Sigma\alpha^{H}_{2} \qquad (N = 16) \qquad (9)$$

$$\log k^{(S)}_{H}(\text{calc}) = (1.8 \pm 0.8) + (0.71 \pm 0.12)\log\ k^{(S)}_{H}(\text{meas}) \qquad (N = 16;\ r^2 = 0.71) \qquad (10)$$

Apparently in contrast with the above conclusion, such a fit is possible but the fit parameters are less well-defined than observed in the previous work on the HAT in flexible bp∪Tyr dyads.[9] Accordingly, the relationship in eq 9 fails to predict the experimental data $k^{(S)}_{H}$ (meas), when using the solvent data in Table 1 and the fitted parameters a and b to recalculate the HAT rate constants, $k^{(S)}_{H}$ (calc).

A plot of the respectively recalculated rate constants against the experimental rate constants is shown in Figure 6. The data are broadly scattered and deviate strongly from the expected 1:1 correlation (full line in Figure 6). The linear regression of the data in terms of eq 10 gives very poor results. In particular, both the slope and the intercept are highly uncertain, a significant deviation from the implications of a 1:1 correlation is evident

(intercept ≫ 0; slope ≠ 1), and the correlation coefficient r^2 of the fit is far from unity. These results are in strong contrast with the outcomes of previous work, wherein we observed a very convincing correlation between the experimental and the recalculated data.[9] We therefore conclude that the effects of the solvents' H-bond acceptor properties and their H-bond donator properties on the HAT reaction of **1** have to be analyzed separately. Again, this is in conflict with the assumption of a common reaction mechanism in all solvents, which is underlying linear-free energy relationships. The implications of this finding on the reaction mechanism of the HAT in protic solvents are discussed in the following.

Mechanistic Implications. Deviations from the predictions of the KSE model in protic solvents have been observed before for some bimolecular HAT reactions from phenols, for example, in the presence of the 2,2-diphenyl-1-picrylhydrazyl radicals. As a rationalization of this deviation, the sequential proton loss electron transfer (SPLET) mechanism has been put forward by Litwinienko and Ingold and, independently, by Foti et al.[4e−h,21] Herein, the higher-than-expected HAT rates from phenols have been attributed to a partial ionization of the phenols to the respective phenoxyl anions and their subsequently fast bimolecular electron transfer. Being a protolytic process in nature, this effect could be totally inhibited by small doses of added acids like acetic acid. It is noted that this mechanism contributes to any significant extent only, when the phenol is very acidic and/or when the overall HAT rate constant is small, that is, when the abstracting radical is only weakly reactive. Our results disfavor significant contributions from the SPLET mechanism, because the HAT rates obtained for **1** in bulk acetic acid are even higher than in MeOH, where the SPLET mechanism should be favored. In agreement with this conclusion, the SPLET mechanism proved insignificant in the bimolecular quenching of ketone triplets by phenol.[7]

In the cited study on the bimolecular triplet quenching the weaker-than-expected reactivity loss in highly H-bond accepting solvents has been tentatively ascribed to contributions from an electron-transfer mechanism, which is driven by the strong solute−solvent interaction and thus partly compensates the reactivity loss implied by the Ingold model. Our results similarly suggest the emergence of a parallel reaction mechanism, which is brought up by specific solute−solvent interactions. Different from the cited work, that was based solely on a study of nonprotic solvents we ascribe the dramatic reactivity gain in protic solvents to a solute−solvent interaction with the solvent functioning as the H-bond donor.

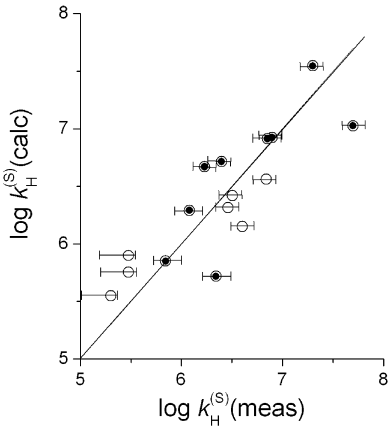

Figure 6. Plot of the recalculated H-atom transfer rate constants, log $k_H^{(S)}$ (calc), computed from eq 9, against the measured H-atom transfer rate constants, log $k_H^{(S)}$ (meas); full line: theoretical 1:1 correlation between measured and calculated rate constants; filled symbols: protic solvents with $\Sigma\alpha_2^H > 0.3$.

SCHEME 4: Suggested Stepwise Electron-Transfer Proton-Transfer Mechanism (ETPT) of the H-Atom Transfer of 1 in Protic Solvents

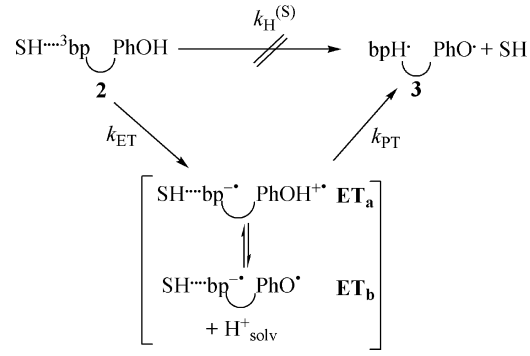

Although we cannot present a definite conclusion at present, mainly due to the lack of direct experimental evidence for ET reaction intermediates, we interpret our data as speaking in favor of a stepwise mechanism for the H-atom transfer of the dyad **1** which is initiated by an electron-transfer step in protic solvents (Scheme 4). This suggestion is in accord with the finding of Canonica et al., that the bimolecular triplet quenching of bp by phenols in aqueous solutions is initiated by electron transfer.[22] In terms of this mechanism the spectroscopic silence of the intermediates $ET_{a/b}$ could be simply attributed to the strong acidity of the phenol cation-radical moiety involved,[23] which should favor a fast intramolecular proton transfer.

We suggest that the reactivity gain in protic solvents, as reflected by the correlation of the HAT rate constants with the H-bond donor ability of the solvent, is due to solvent effects on the redox properties of the dyad **1**. In particular, we suggest that specific solvation of the benzophenone and the tyrosine moiety reduces both the reduction potential of the former and the oxidation potential of the latter. Such effects of specific solvation by H-bonding on the redox properties of a solute are not uncommon in electrochemistry. Literature data of direct relevance for the present study are strongly in favor of a direct correlation of the redox properties of aromatic ketones and phenols with specific solvation effects in terms of hydrogen bonding to and from the solvent.[24−29] The solvent-dependence of the electrochemical potentials thus is expected to have important implications on the thermodynamics of the anticipated ET reaction from Tyr to the triplet-excited bp.

Conclusions

Solvent effects on the rates of intramolecular H-atom transfer have been commonly observed in ketone-phenol dyads.[10,30,31] The relative order of the rates has been tentatively ascribed to the H-bond acceptor properties of the surrounding medium but was based on data in only a few solvents.[10,30b] In a broad survey we recently showed that this single-parameter approach actually sufficed to explain the solvent dependence of the intramolecular HAT in two diastereomeric bp∪Tyr dyads.[9] In the current study on the intramolecular hydrogen-atom transfer of the bp∪Tyr dyad **1** in eighteen solvents and solvent mixtures, we provide evidence that, besides the propensity of the solvent to accept H-bonds, its capabilities to act as also an H-bond donor need to be considered. The contrasting solvent dependencies of the H-atom transfer rate constants in protic and nonprotic solvents are best interpreted as being due to fundamentally different

H-atom transfer mechanisms in the respective solvents. Our results suggest that, at least for intramolecular HAT reactions, the solvation of the abstracting species needs to be considered a priori as important as that of the H-donating species.

The H-transfer rates in nonprotic solvents are limited by the accessibility of free, that is, not H-bonded, tyrosine. This effect is accounted for in an intramolecular model for a kinetic solvent effect. The comparison of a such-derived prediction equation with one obtained by Ingold et al. for bimolecular H-atom transfer reactions[4d] points to a more fundamental similarity of the H-transfer processes irrespective of the molecularity of the reaction. Notably, this simple model fails to explain the data obtained in protic solvents. The kinetic data obtained in protic media follow a correlation with the H-bond donor ability of the solvent. Significant deviations from this correlation are only noticed for solvents of low bulk permittivity, that is, in chlorohydrocarbon solutions. We suggest that the H-atom transfer in protic solvents likely follows a stepwise electron-transfer proton-transfer sequence. Further work is needed to put this suggestion to the test and to rationalize the structural features which determine the contributions from the competing mechanistic paths.

Acknowledgment. This work was supported by COST Chemistry CM0603. G.L.H. was a Fulbright Scholar at AMU. The authors thank Prof. B. Abel and Dr. R. Hermann (University Leipzig, Germany) for technical support with the LFP equipment. The calculations were performed at the Poznan Supercomputer Center PCSS. This paper is Document No. NDRL-4797 from the Notre Dame Radiation Laboratory, which is supported by the Office of Basic Energy Sciences of the U.S. Department of Energy.

References and Notes

(1) (a) Burton, G. W.; Doba, T.; Gabe, E. J.; Hughes, L.; Lee, L.; Prasad, L.; Ingold, K. U. *J. Am. Chem. Soc.* **1985**, *107*, 7053–7065. (b) Foti, M. C. *J. Pharm. Pharmacol.* **2007**, *59*, 1673–1685. (c) Stubbe, J.; van der Donk, W. A. *Chem. Rev.* **1998**, *98*, 705–762. (d) Hoganson, C. W.; Tommos, C. *Biochim. Biophys. Acta* **2004**, *1655*, 116–122.

(2) Recent examples: (a) Mayer, J. M.; Hrovat, D. A.; Thomas, J. L.; Borden, W. T. *J. Am. Chem. Soc.* **2002**, *124*, 11142–11147. (b) Chang, C. J.; Chang, M. C. Y.; Damrauer, N. H.; Nocera, D. G. *Biochim. Biophys. Acta* **2004**, *1655*, 13–28. (c) Mayer, J. M. *Annu. Rev. Phys. Chem.* **2004**, *55*, 363–390. (d) Rhile, I. J.; Markle, T. F.; Nagao, H.; DiPasquale, A. G.; Lam, O. P.; Lockwood, M. A.; Rotter, K.; Mayer, J. M. *J. Am. Chem. Soc.* **2006**, *128*, 6075–6088. (e) DiLabio, G.; Johnson, E. R. *J. Am. Chem. Soc.* **2007**, *129*, 6199–6203. (f) Markle, T. F.; Rhile, I. J.; DiPasquale, A. G.; Mayer, J. M. *Proc. Natl. Acad. Sci.* **2008**, *105*, 8185–8190.

(3) (a) Jasperse, C. P.; Curran, D. P.; Fevig, T. L. *Chem. Rev.* **1991**, *91*, 1237–1286. (b) Barclay, L. R. C.; Edwards, C. E.; Vinqvist, M. R. *J. Am. Chem. Soc.* **1999**, *121*, 6226–6231.

(4) (a) Avila, D. V.; Ingold, K. U.; Lusztyk, J. *J. Am. Chem. Soc.* **1995**, *117*, 2929–2930. (b) Valgimigli, L.; Banks, J. T.; Ingold, K. U.; Lusztyk, J. *J. Am. Chem. Soc.* **1995**, *117*, 9966–9971. (c) Banks, J. T.; Ingold, K. U.; Lusztyk, J. *J. Am. Chem. Soc.* **1996**, *118*, 6790–6791. (d) Snelgrove, D. W.; Lusztyk, J.; Banks, J. T.; Mulder, P.; Ingold, K. U. *J. Am. Chem. Soc.* **2001**, *123*, 469–477. (e) Litwinienko, G.; Ingold, K. U. *J. Org. Chem.* **2003**, *68*, 3433–3438. (f) Litwinienko, G.; Ingold, K. U. *J. Org. Chem.* **2004**, *69*, 5888–5896. (g) Litwinienko, G.; Ingold, K. U. *J. Org. Chem.* **2005**, *70*, 8982–8990. (h) Litwinienko, G.; Ingold, K. U. *Acc. Chem. Res.* **2007**, *40*, 222–230.

(5) MacFaul, P. A.; Ingold, K. U.; Lusztyk, J. *J. Org. Chem.* **1996**, *61*, 1316–1321.

(6) Koner, A. L.; Pischel, U.; Nau, W. M. *Org. Lett.* **2007**, *9*, 2899–2902.

(7) Galian, R. E.; Litwinienko, G.; Perez-Prieto, J.; Ingold, K. U. *J. Am. Chem. Soc.* **2007**, *129*, 9280–9281.

(8) (a) Das, P. K.; Encinas, M. V.; Scaiano, J. C. *J. Am. Chem. Soc.* **1981**, *103*, 4154–4162. (b) Das, P. K.; Encinas, M. V.; Steenken, S.; Scaiano, J. C. *J. Am. Chem. Soc.* **1981**, *103*, 4162–4166.

(9) Hörner, G.; Hug, G. L.; Lewandowska, A.; Kazmierczak, F.; Marciniak, B. *Chem.—Eur. J.* **2009**, *15*, 3061–3064.

(10) Hörner, G.; Hug, G. L.; Pogocki, D.; Filipiak, P.; Bauer, W.; Grohmann, A.; Lämmermann, A.; Pedzinski, T.; Marciniak, B. *Chem.—Eur. J.* **2008**, *14*, 7913–7929.

(11) Abraham, M. H. *Chem. Soc. Rev.* **1993**, 73–83.

(12) (a) Hermann, R.; Malahaxmi, G. R.; Jochum, S.; Naumov, S.; Brede, O. *J. Phys. Chem. A* **2002**, *106*, 2379–2389. (b) Pedzinski, T.; Markiewicz, A.; Marciniak, B. *Res. Chem. Intermed.* **2009**, in press.

(13) Bensasson, R. V.; Gramain, J.-C. *J. Chem. Soc. Faraday Trans. 1* **1980**, *76*, 1801–1810.

(14) Das, P. K.; Bhattacharyya, S. N. *J. Phys. Chem.* **1981**, *85*, 1391–1395.

(15) Wagner, P. J.; Pabon, R.; Park, B.-S.; Zand, A. R.; Ward, D. L. *J. Am. Chem. Soc.* **1994**, *116*, 589–596.

(16) Hofmann, R.; Schleyer, P. R.; Schaefer III, H. F. *Angew. Chem. Int. Ed.* **2008**, *47*, 7164–7167.

(17) (a) Kobayashi, J.; Nagai, U. *Biopolymers* **1978**, *17*, 2265–2277. (b) Kobayashi, J.; Higashijima, T.; Sekido, S.; Miyazawa, T. *Int. J. Peptide Protein Res.* **1981**, *17*, 486–494. (c) Kobayashi, J.; Higashijima, T.; Miyazawa, T. *Int. J. Peptide Protein Res.* **1984**, *24*, 40–47.

(18) Pachler, K. G. R. *Spectrochim. Acta* **1964**, *20*, 581–587.

(19) Abraham, M. H.; Grellier, P. L.; Prior, D. V.; Morris, J. J.; Taylor, P. J. *J. Chem. Soc., Perkin Trans. 2* **1990**, 521–529.

(20) Zheng, J.; Fayer, M. D. *J. Am. Chem. Soc.* **2007**, *129*, 4328–4335.

(21) Foti, M. C.; Daquino, C.; Geraci, C. *J. Org. Chem.* **2004**, *69*, 2309–2314.

(22) Canonica, S.; Hellrung, B.; Wirz, J. *J. Phys. Chem. A* **2000**, *104*, 1226–1233.

(23) Bordwell, F. G.; Cheng, J.-P. *J. Am. Chem. Soc.* **1991**, *113*, 1736–1743.

(24) Wagner, P. J.; Truman, R. L.; Puchalski, A. E.; Wake, R. *J. Am. Chem. Soc.* **1986**, *108*, 7727–7738.

(25) Barwise, A. J. G.; Gorman, A. A.; Leyland, R. L.; Smith, P. G.; Rodgers, M. A. *J. Am. Chem. Soc.* **1978**, *100*, 1814–1820.

(26) (a) Gupta, N.; Linschitz, H. *J. Am. Chem. Soc.* **1997**, *119*, 6384–6391. (b) Jonsson, M.; Houmam, A.; Jocys, G.; Wayner, D. D. M. *J. Chem. Soc., Perkin Trans. 2* **1999**, 425–429.

(27) Lucarini, M.; Mugnaini, V.; Pedulli, G. F.; Guerra, M. *J. Am. Chem. Soc.* **2003**, *125*, 8318–8329.

(28) Harriman, A. *J. Phys. Chem.* **1987**, *91*, 6102–6104.

(29) Nakanishi, I.; Kawashima, T.; Ohkubo, K.; Kanazawa, H.; Inami, K.; Mochizuki, M.; Fukuhara, K.; Okuda, H.; Ozawa, T.; Itoh, S.; Fukuzumi, S.; Ikota, N. *Org. Biomol. Chem.* **2005**, *3*, 626–629.

(30) (a) Miranda, M. A.; Lahoz, A.; Martinez-Manez, R.; Bosca, F.; Castell, J. V.; Perez-Prieto, J. *J. Am. Chem. Soc.* **1999**, *121*, 11569–11570. (b) Perez-Prieto, J.; Lahoz, A.; Bosca, F.; Martinez-Manez, R.; Miranda, M. A. *J. Org. Chem.* **2004**, *69*, 374–381.

(31) (a) Scaiano, J. C.; McGimpsey, W. G.; Leigh, W. J.; Jakobs, S. *J. Org. Chem.* **1987**, *52*, 4540–4544. (b) Leigh, W. J.; Lathioor, E. C.; St. Pierre, M. J. *J. Am. Chem. Soc.* **1996**, *118*, 12339–12349. (c) Lathioor, E. C.; Leigh, W. J. *Can. J. Chem.* **2001**, *79*, 1851–1863.

JP901740Z